

# Hybrid AI for Enhanced Voltage Control in Three-Phase Boost Rectifiers

Alireza Khoshsaadat<sup>1</sup> | Arash Khoshooei<sup>2</sup> | Mohammad Abedini\*<sup>3</sup> | Mohammadreza Mirzaei<sup>4</sup>

<sup>1</sup>Department of Electrical Engineering, Shahid Beheshti University, Tehran, Iran

<sup>2</sup>Assistant Professor, Jundi-Shapur University of Technology, Dezful, Iran,

<sup>3</sup> Department of Electrical Engineering, Faculty of Engineering, Ayatollah Boroujerdi University, Boroujerd, Iran

<sup>4</sup> Master of Electrical Engineering, Planning and Management of Electrical Energy Systems, Ayatollah Boroujerdi University, Iran

\* Corresponding Author: [m.abedini@abru.ac.ir](mailto:m.abedini@abru.ac.ir)

| Article Info  | ABSTRACT   |
|---|--|
| <p><b>Article type:</b><br/>Research Article</p> <p><b>Article history:</b><br/>Received: 14-August-2024<br/>Received in revised form:<br/>08-November-2024<br/>Accepted: 30-November-2024<br/>Published online: 22-Dec-2025</p> <p><b>Keywords:</b><br/>ANFIS Controller,<br/>Voltage-Oriented Control,<br/>Direct Power Control,<br/>Rectifier.</p> | <p>Three-phase boost rectifier is a Voltage-Source Converter that converts three-phase AC input voltage to a higher DC voltage. In this paper, an artificial intelligent-based system, with learning and adapting capability, is proposed for utilizing in the two voltage-based control methods of rectifiers, with the names of Voltage Oriented Control (VOC) and Direct Power Control (DPC). For implementation of this intelligent controller, a hybrid structure of the Fuzzy Logic (FL) and Neural Networks (NNs) that named as Adaptive Network-based Fuzzy Inference System (ANFIS) is applied. Among the common network training algorithms, the error back propagation algorithm is known as the most common solution by providing an efficient computational method. Thus this method is used to design the training process of the controller. According to the results, this neuro-fuzzy-based control model is applicable in both VOC and DPC methods and increases the quality of the output current and DC voltage with low ripple, short settling time and also dynamic operation. Implementation of the proposed controller is simple and requires only 49 fuzzy rules. Compared to other similar controllers with NN and FL, it has fewer layers and its accuracy is suitable. To evaluate of the designed controller performance, it is simulated and applied in both VOC and DPC systems and the results are compared with PID Controller counterpart.</p> |

## I. Introduction

Three-phase Pulse Width Modulation (PWM) rectifiers are workhorses in power electronics, converting AC input into DC output using either voltage-based or virtual flux-based control methods. These control methods categorized in two main categories: voltage-based and virtual flux-based. Voltage-based control, like Voltage-Oriented Control (VOC) and Direct Power Control (DPC), directly utilizes the line voltage vector for regulation and control. In contrast, virtual flux-based control, by introducing Virtual Flux Direct Power Control (VF-DPC), calculates a virtual voltage reference, eliminating the need for physical voltage sensors. VF-DPC achieves this target by replacing the line voltage vector with a virtual flux estimation and leading to reduced harmonic distortion and a more sinusoidal line current in many cases. Virtual Flux-Oriented Control (VFOC) is another approach that leverages virtual flux for DC voltage control [1, 2].

While all control methods for three-phase PWM rectifiers aim for near-unity power factor and sinusoidal input current, they achieve this approaches with distinct merits and limitations.

VOC and VFOC prioritize static and dynamic performance. They achieve this by using an internal current control loop as a crucial element in their operation.

DPC and VF-DPC take a different approach. They focus on instantaneous control of direct and reactive power, eliminating the need for an internal current control loop and a dedicated PWM block. Instead, they rely on a switching table based on the difference between reference and estimated power values to select the appropriate switching strategy [3, 4, 5].

Sliding Mode Direct Power Control (SMC-DPC) is a robust control technique for Doubly Fed Induction Generators (DFIGs) [6, 7, 8]. It boosts fast power convergence and resilience against parameter variations, but

can introduce some of power chattering [9].

Double synchronous reference frame controllers, explored in [10, 11]. It offers improved performance through the addition of a decoupling network to manage unwanted current oscillations. Literature also discuss variations of switching tables for active front-ends to enhance performance (e.g., [12, 13]), but the methodology for their formation is often lacking detailed explanation.

According to the literature review and combination of artificial intelligent systems, this paper proposes a novel control method for voltage-based methods (VOC and DPC) in three-phase PWM rectifiers. The core of this method is an Adaptive Network-based Fuzzy Inference System (ANFIS) controller that combines the strengths of Neural Network (NN) and Fuzzy Logic (FL). This hybrid approach offers increased flexibility and adaptability to change system conditions.

The ANFIS controller utilizes a single NN architecture with 5 layers to implement the entire fuzzy system. A learning algorithm based on Forward Signal and Backward Error Back-Propagation (FSBEBP) is used to adjust the parameters within the Sugeno-based fuzzy controller and optimize system performance.

The ANFIS controller uses a 5-layer NN architecture to implement the key functionalities of a FL system. The hidden layers within this network act as both membership function mappers and a fuzzy inference engine. The underlying fuzzy rules, based on engineering knowledge of the controlled rectifier, are translated into this NN structure.

The proposed controller utilizes a specific architecture with 2, 14, 49, 49, and 1 nodes in each of the 5 layers. This architecture allows the ANFIS controller to effectively implement the fuzzy control strategy. The proposed ANFIS controller is evaluated for both VOC and DPC strategies in rectifier control. The results demonstrate its superiority over traditional PID controllers. Unlike PID controllers, which require manual adjustments for varying system conditions, the ANFIS controller can inherently adapt, offering significant advantages.

## II. Neural Networks, Fuzzy Logic, and Hybrid Neuro-Fuzzy Systems

Both FL and NNs are powerful tools for building intelligent systems, but they have distinct characteristics that should be considered.

### A. Neural Network

Artificial NNs are a well-known machine learning technique for processing data through analytical layers. Similar to neurons in the human brain, NNs are composed of interconnected neurons, which are called nodes. These nodes are connected to each other through axons called weights

that their values are in range of 0-1. In a NN system, nodes are placed together and form layers.

Using of NNs has their advantages and disadvantages. Advantages of NNs are as below [14, 15]:

- Has redundant nature and thus, when a part of the NN fails, it can continue processing based on their parallel nature;
- Can perform non-linear process that a linear system cannot;
- Has high robustness against disturbances due of learning ability;

And disadvantages of NNs are as below:

- Cumbersome mass of calculation;
- Difficulty in determining the optimum architecture, such as number of neurons and layers.

### B. Fuzzy Logic

Unlike deterministic sets, a fuzzy set allows an element to belong relatively to a set. This relative membership is defined by the degree of membership and is indicated by the degree of membership can take a value between 0 (for an element that does not belong to the set at all) and 1 (for an element that completely belongs to the set). The set membership function is the relationship between the elements of the set and their degree of belonging. General advantages of the FL systems are:

- Human-like reasoning: FL can handle uncertainties and express knowledge using linguistic variables, making it easier to understand and integrate expert knowledge into the system.

- Adaptability: FL systems can be easily extended by adding new rules, allowing for knowledge-based growth without significant structural changes.

- Reduced overshoot and oscillation: FL systems can often achieve smooth control outputs with low overshoot and oscillation.

And disadvantages of FL systems are:

- Limited generalization: FL systems struggle with situations outside their defined rule base, lacking the ability to generalize effectively to unseen scenarios.

- Expert Dependence: Designing effective fuzzy systems requires expert knowledge to define the appropriate rules, potentially limiting their accessibility.

For understanding FL, Fig. 1 illustrates a typical fuzzy system with four key components:

- 1) Fuzzification Unit: this unit transforms crisp (exact) inputs into fuzzy values, indicating the degree of their membership in various fuzzy sets.

- 2) Knowledge Base: this core element stores the fuzzy rules that govern system behavior. It's essentially a collection of expert knowledge expressed in linguistic terms.

- 3) Inference Engine: this unit applies the fuzzy rules from the knowledge base to the fuzzified inputs, determining the appropriate control action. It mimics human decision-making to some extent.

4) Defuzzification Unit: this unit converts the inferred fuzzy control values back into crisp outputs that can be applied to the system.

By combining these components, FL systems can provide robust control strategies even with imprecise or incomplete information.

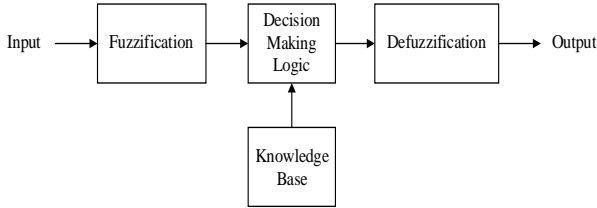


Fig. 1. Basic model of a FL system.

### C. Hybridization of FL and NN

In this study, in order to design a suitable controller for the switching process in the rectifier, an adaptive neural fuzzy inference system is used. This system is a modeling framework that is presented as a combination of FL and artificial NN. This hybrid model is presented in order to overcome the weaknesses in both FL and artificial NN methods. In fact, inspired by fuzzy systems, the initial knowledge is shown in a set of constraints in order to reduce the optimization search space. While the structured network using backpropagation is inspired by the artificial NN. In this model, artificial NN is used to adjust the membership functions.

Also, the presence of non-linear membership functions in the neuro-fuzzy method leads to a significant reduction in the cost of implementing a simple plan based on the rules and memory used; therefore, it is clear that the combination of NN and fuzzy systems reduces the limitations of each of these two methods and leads to the proposal of a data mining method to solve complex engineering problems. Adaptive neural fuzzy inference system (ANFIS) is one of the well-known methods in the simultaneous combination of NN and fuzzy systems [24]. This method is used to identify the behavior of non-linear systems using the set of input and output data defined for the model. Adaptive neural fuzzy inference system is a structured model of fuzzy inference system. The used ANFIS is based on Sugeno fuzzy method to make fuzzy rules using input and output data defined. In the part IV, more detailed of this design will be represented.

## III. Model of Three-phase Rectifier, VOC and DPC Control Strategies

### A. Model of a 6-switches Three-phase Rectifier

Fig. 2 depicts a typical 6-switches three-phase PWM rectifier circuit with a specific switch configuration. A universal bridge topology for arrangement of the switch is applied in Fig. 2. By this architecture, unity power factor and bidirectional energy flow can be achieved.

The figure presents the following elements and subsystems:

- 1) Input phase voltages:  $U_a, U_b, U_c$ .
- 2) Filter components:  $L$  (inductance) and  $R$  (resistance) of the filter.
- 3) Input and switching elements:  $A, B,$  and  $C$  (input phases) and  $S_a, S_b, S_c$  (switching legs for the three-phase rectifier).
- 4) Output and load:  $U_{dc}$  (DC output voltage),  $C$  (filter capacitor), and  $R_L$  (equivalent load resistance).

Equation (1) will present the mathematical model of this three-phase PWM rectifier in the synchronous rotating frame.

$$L \frac{di_d}{dt} = u_d - Ri_d - \omega Li_q - S_d U_{dc} \quad (1)$$

$$L \frac{di_q}{dt} = u_q - Ri_q + \omega Li_d - S_q U_{dc}$$

And using the KCL law in the output node:

$$C \frac{dU_{dc}}{dt} = i_d S_d + i_q S_q - \frac{U_{dc}}{R_L} \quad (2)$$

where the d and q indices are the transformed variable from abc phases to the d-q frame. This model can be easily implemented using SIMULINK [2].

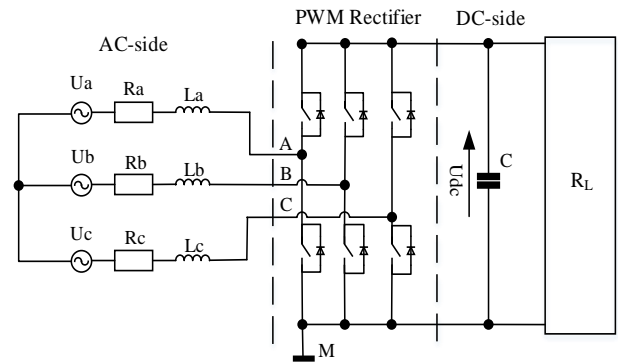


Fig. 2. Three-phase PWM rectifier circuit model.

### B. Model of VOC strategy

The VOC method is based on the some transformation from three-phase a, b, c reference system to a synchronous rotating reference frame d-q, through a two phase stationary reference system  $\alpha$ - $\beta$ . With these transformations, the control voltages remain constant and become DC values and the control process is simplified.

As mentioned previously, closed-loop current control is used in this method [2]. The VOC has some advantages as:

- . Fixed frequency method can be applied for switching process.
- . Advanced PWM pattern can be used.
- . Cheaper A/D converter is used.

Meanwhile, VOC has some disadvantages such as:

- . Relative complex algorithm.
- . Lower power factor in comparison with other methods.
- . Decoupling structure for controlling of the active and reactive power is required [3].

Implementation of the VOC model for rectifier control has four main stages as below:

- 1) PWM unit: that controls the pulse width of the switches of the rectifier. This work performs with comparing of the triangular carrier with the modulator sinusoidal wave that comes from decoupled controller unit with the  $V_{dc}/2$  amplitude.
- 2) Decoupled controller unit: in this unit, the voltage controller produces the reference  $i_d$  for the decoupled current controller at first (references  $i_q$  is zero because rectifier has no reactive power exchanging with the grid); then using references of the  $i_d$  and  $i_q$ , proper control signal will produce with the two decoupled controllers. This unit is demonstrated in the Fig. 3. Also, an ANFIS controller applied for this part of the system is applied that will be represented in the next section.
- 3) Phase Locked Loop (PLL) unit: This unit gives the voltage angle of the three phase system, and this angle was used for all abc to d-q transformation blocks in the model.
- 4) Rectifier unit: model of this unit represented in Fig. 2. Putting together of the aforementioned building blocks of the VOC, the block-diagram of the controlled rectifier is represented in Fig. 4.

Fig. 4 has 4 major parts, as mentioned previously, and also two three-phase to d-q frame transformer blocks.

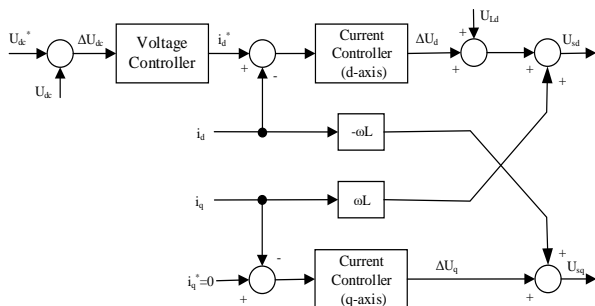


Fig. 3. SIMULINK diagram of the decoupled controller unit.

### C. Model of DPC strategy

Direct Power Control (DPC) is a control method for three-phase PWM rectifiers that prioritizes simplicity and efficiency. Unlike other methods, DPC bypasses the need for an internal current control loop and complex coordinate transformations. Instead, it relies on readily available information like network voltage position and power errors to directly select the appropriate voltage vector from a predefined switching table [6, 7]. This approach streamlines the control process and enables independent control of active

and reactive power (decoupled control) [8, 9]. Generally,

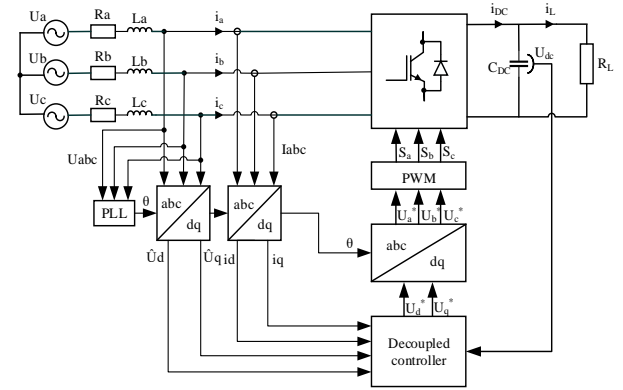


Fig. 4. The VOC method for PWM rectifier.

DPC has advantages as:

- . PWM block system, current controllers, and coordinate transformation are not needed.
- . Has decoupled active and reactive power control and good dynamic response and a simple algorithm.
- . Can estimate instantaneous variables appropriately.

Also, DPC has some disadvantages such as:

- . Variable switching frequency.
- . Fast and complicated processor and also A/D converter are required.

For implementing of the DPC method we have 4 major parts as below:

- 1) Instantaneous power estimator unit: this unit estimate the active and reactive power of the line based on the voltage of line by the product of the three-phase voltages and currents. This work need to the high value of the line inductance and sampling frequency, and also depends on the switching states. The below equations represented the instantaneous active and reactive powers:

$$p = L \left( \frac{di_a}{dt} i_a + \frac{di_b}{dt} i_b + \frac{di_c}{dt} i_c \right) + U_{dc} (S_a i_a + S_b i_b + S_c i_c) \quad (3)$$

$$q = \frac{1}{\sqrt{3}} \left\{ 3L \left( \frac{di_a}{dt} i_c - \frac{di_c}{dt} i_a \right) - U_{dc} (S_a (i_b - i_c) + S_b (i_c - i_a) + S_c (i_a - i_b)) \right\}$$

These estimated powers are compared with their reference values and the produced errors are fed to fixed band hysteresis comparators to generate two digital signals  $dp$  and  $dq$ . For the unity power factor operation, the reference value of the reactive power  $q_{ref}$  is set to zero.

- 2) Switching table unit: The switching pattern for the rectifier switches is stored in a lookup table (LUT) within this unit. This table influences factors such as instantaneous power and current ripple, switching frequency, and overall dynamic performance. The LUT values are based on:

- . Digitized signals  $dp$  and  $dq$  representing the instantaneous errors of active and reactive power, respectively (provided by hysteresis comparators).

- . Power source voltage vector position.

Typically, the voltage vectors is divided into 12 sectors. Table I illustrates the lookup table layout with predefined

switching functions ( $S_a, S_b, S_c$ ) assigned to each sector.

TABLE I SWITCHING LOOK-UP TABLE.

| dp | dq | $\gamma_1$ | $\gamma_2$ | $\gamma_3$ | $\gamma_4$ | $\gamma_5$ | $\gamma_6$ | $\gamma_7$ | $\gamma_8$ | $\gamma_9$ | $\gamma_{10}$ | $\gamma_{11}$ | $\gamma_{12}$ |
|----|----|------------|------------|------------|------------|------------|------------|------------|------------|------------|---------------|---------------|---------------|
| 1  | 0  | 101        | 111        | 100        | 000        | 110        | 111        | 010        | 000        | 011        | 111           | 001           | 000           |
|    | 1  | 111        | 111        | 000        | 000        | 111        | 111        | 000        | 000        | 111        | 111           | 000           | 000           |
| 0  | 0  | 101        | 100        | 100        | 110        | 110        | 010        | 010        | 011        | 011        | 001           | 001           | 101           |
|    | 1  | 100        | 110        | 110        | 010        | 010        | 011        | 011        | 001        | 001        | 101           | 101           | 100           |

3) Controller unit: this unit uses the error between DC output voltage and output DC reference voltage, as input. The reference of the active power for hysteresis active power controller is obtained from this unit. Our ANFIS controller is applied instead of this controller unit.

4) Rectifier unit: as explained for the VOC method, model of this unit is represented in the previous sections is used for DPC method either. In Fig. 5, the block-diagram of the DPC method is represented.

#### IV. Design of ANFIS

The set of rules considered for a fuzzy inference system of the Takagi-Sugno-Kang type is expressed as if-then rules as follows [18,19]:

$$\text{*IF } X_i \text{ is } A_i \text{ and } Y_i \text{ is } B_i, \text{ THEN } f_k = p_k X_i + q_k Y_i + r_k \text{*}$$

The rule-base as a look-up-table is provided to define the expert's knowledge for applying of the FL controller arrangement. If "Z" is the form of the linear syntax of the "X" and "Y", this type of fuzzy rules named as "sugeno" that given in Fig. 4 with seven sets Negative Big (NEB), Negative Medium (NEM), Negative Small (NES), Zero (ZE), Positive Small (POS), Positive Medium (POM), and Positive Big (POB) as the fuzzy values [17]. The number of first layer nodes is determined using the number of inputs and the number of membership functions for each input. But the number of nodes in other layers depends on the number of rules in the fuzzy rule set. Table II shows the provided rules as inference engine. Although the number of rules can be increased, minimum rules have been used to reduce calculations in controller design. For implementing of the controlling system, the error between output DC voltage and reference DC voltage and derivative of that (shown with "e" or "X<sub>1</sub>", and "de" or "X<sub>2</sub>" respectively) are considered as the two input of the FL controller. Every of two fuzzified input is divided to the 7 fuzzy confine. Finally noting to the two inputs and scaling of them, we have output table with 49 arrays for inference system. This process are implemented using 5 layer NN, in ANFIS architecture, for partaking from parallel processing and learning ability of the NN, neighbor

to the inference capability of the FL. Fig. 7 demonstrations the organization of the offered ANFIS, which has been used as controller. As shown in Fig. 5, architecture of the NN has five layers as following:

1) First layer: The first layer: each node in this layer determines a degree of membership for the inputs. In fact, this layer will convert any input value into a specific fuzzy range. The fuzzy function in this layer can be expressed as follows:

$$O_{ij}^1 = \mu_{ij}(x_i) \quad i=1,2, \quad j=1,2,\dots,14; \quad (4)$$

where,  $\mu_{ij}$  is equal to  $j^{\text{th}}$  the membership function for the input  $x_i$  and  $O_{ij}^1$  is the output of the node  $ij$ .

Due to the good performance and satisfactory performance of the triangular membership function in various engineering applications, the membership function used in this study is a triangular type. The mathematical relationship of this membership function is as follows:

$$\mu(x) = \max\left[\min\left(\frac{x-a}{b-a}, \frac{c-x}{c-b}\right), 0\right]; \quad (5)$$

where a, b and c are the set of parameters.

2) Second layer: Each node in this layer (k), which is presented as circular nodes ( $\Pi$ ), (See Fig. 7), produces the output using the received inputs.

$$O_k^2 = \mu_{e_1}(X_1^2) \mu_{e_2}(X_2^2); \quad k=1,\dots,49; e_1, e_2=1,\dots,7; \quad (6)$$

3) Third layer: In layer of node  $k^{\text{th}}$ , the ratio of the fire power of the law  $k^{\text{th}}$  to the fire power of the whole law has been determined as follows [22]:

$$O_i^3 = \overline{W_k} = \frac{W_k}{\left(\sum_{k=1}^{k=49} W_k\right)}; \quad i, k=1,2,\dots,49; \quad (7)$$

4) Fourth layer: Each node in this layer acts as a weighted output of the fuzzy inference system as follows:

$$O_i^4 = \overline{W_k} f_k = \overline{W_k} (p_k X_1 + q_k X_2 + r_k), k = 1, \dots, 49; \quad (8)$$

Where  $W_k$  is the output of the non-fuzzy layer and  $f_k$  is the output of the rule  $M^{th}$  of the Takagi-Sugeno-Kang fuzzy inference system. Also,  $p_k, q_k$  and  $r_k$  are the set of parameters. 5) Fifth layer: In this layer, the single circular node,  $\Sigma$ , calculates all outputs as the sum of all inputs as follows:

$$O_1^5 = \frac{k=49}{\sum_{k=1}} \overline{W_k} f_k \quad (9)$$

This node is only used because we have only one output. Noting that the square nodes which are adaptive nodes have control parameters while the circle nodes which are fixed node has none.

The proposed ANFIS controller utilizes a learning algorithm called Forward Signal and Backward Error Back-Propagation (FSBEBP) to adjust its internal parameters. This algorithm works in two stages:

- 1) Forward Pass: In this stage, the input vector is fed through the ANFIS network layer by layer. Each layer performs its designated calculations, ultimately producing an output value.
- 2) Backward Pass: Here, the error between the actual output and the desired output is calculated. This error is then propagated backward through the network layer by layer. Similar to traditional Backpropagation, the FSBEBP algorithm uses the gradient descent technique to modify the network's internal parameters (premise parameters) based on the calculated errors. This process aims to minimize the overall error and improve the controller's performance [20-22].

So it can be written as:

$$\frac{\partial E_k}{\partial g_i} = \eta \frac{\partial E_k}{\partial O_k} \frac{\partial O_k}{\partial g_i} = \eta (O_k - y_k) \frac{\partial O_k}{\partial g_i} \quad (10)$$

where,  $\eta$  is the learning rate of the NN-based network,  $g_i$  is the consequence parameter and  $O_i$  is the output of  $i$ -th layer. Also,  $E_k$  is the cost function of the error and can be calculated as follows:

$$E_k = \frac{1}{2} (d_k - O_k)^2 \quad (11)$$

where,  $d_k$  is the desired response of the  $k$ -th layer and  $O_k$  is the output of the  $k$ -th layer. The error rate for consequence parameters can be expressed as follows:

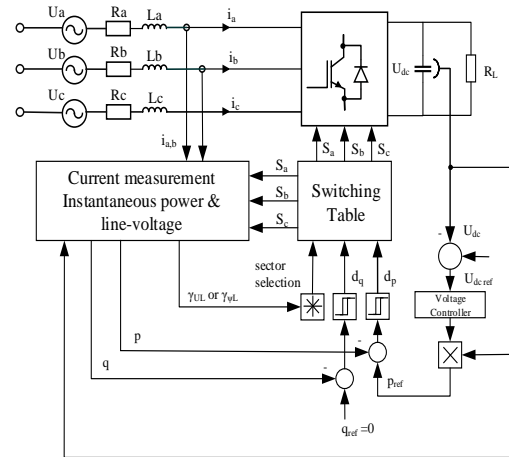


Fig. 5. Block diagram of the DPC of PWM rectifier.

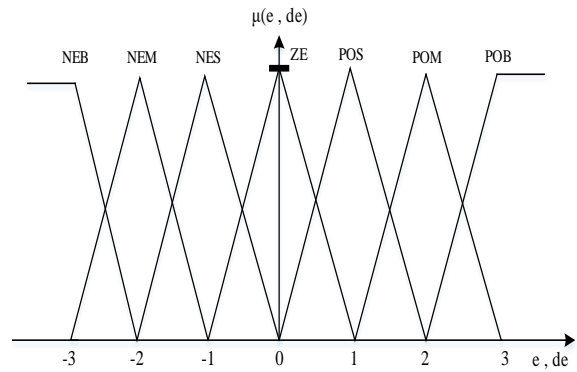


Fig. 6. Membership functions for the error between the output DC voltage and reference DC voltage and derivative of the error, as two inputs of the fuzzy system.

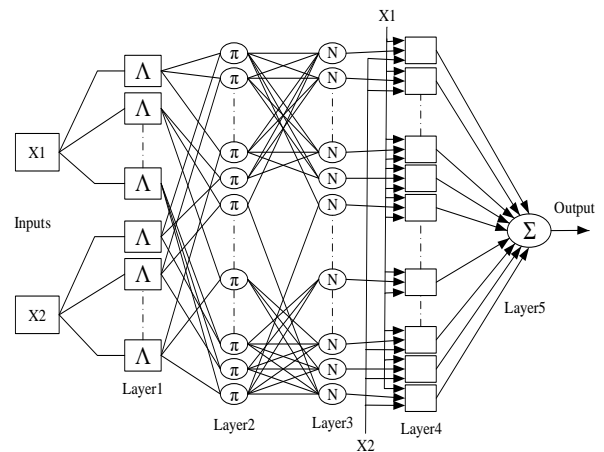


Fig. 7. Architecture of the proposed ANFIS controller (X1 and X2 are  $e$  and  $de$ ).

TABLE II FUZZY INFERENCE ENGINE TABLE.

| e  | NEB    | NE<br>M | NES | ZE      | POS     | PO<br>M | POB    |        |
|----|--------|---------|-----|---------|---------|---------|--------|--------|
| de | NEB    | POB     | POB | PO<br>M | POS     | POS     | POS    | Z<br>E |
|    | NEM    | POB     | POM | POS     | POS     | POS     | Z<br>E | NES    |
|    | NES    | PO<br>M | POS | ZE      | ZE      | Z<br>E  | NES    | NEM    |
|    | Z<br>E | PO<br>M | POS | ZE      | ZE      | Z<br>E  | NES    | NEM    |
|    | POS    | PO<br>M | POS | ZE      | ZE      | ZE      | NES    | NEM    |
|    | POM    | POS     | ZE  | POS     | NES     | NES     | NEM    | NEB    |
|    | POB    | ZE      | NES | NES     | NE<br>S | NE<br>M | NEB    | NEB    |

$$\frac{\partial E_k}{\partial g_c} = \frac{\partial E_k}{\partial O_5} \frac{\partial O_5}{\partial O_4} \frac{\partial O_4}{\partial g_c} \quad (12)$$

THEN-part of the Sugeno rules can be calculated as:

$$\frac{\partial O_4}{\partial p_k} = \overline{W_k} X, \quad \frac{\partial O_4}{\partial q_k} = \overline{W_k} Y, \quad \frac{\partial O_4}{\partial r_k} = \overline{W_k}; \quad (13)$$

where,  $k$  is the suggested rule.

For updating of the premise parameters we will have:

$$\frac{\partial E_k}{\partial g_p} = \eta \frac{\partial E_k}{\partial O_5} \frac{\partial O_5}{\partial O_4} \frac{\partial O_4}{\partial O_3} \frac{\partial O_3}{\partial O_2} \frac{\partial O_2}{\partial O_1} \frac{\partial O_1}{\partial g_p} \quad (14)$$

where,  $g_p$  is the premise parameter. With computation of the each section of the equation we have:

$$\frac{\partial E_k}{\partial g_c} = \eta (O_5 - d_5) f_k \frac{\sum_{j=1}^{j=49} w_j^{-w_i} \partial (\prod_{k=1, k \neq m}^{49} T_k)}{(\sum_{j=1}^{j=49} w_j)^2} \frac{\partial O_1}{\partial T_m} \frac{\partial O_1}{\partial g_p} \quad (15)$$

where  $\frac{\partial O_1}{\partial g_p}$  is the derivative of the output of the first layer.

This layer maps its output to the three parameters (a, b, and c) of a triangular membership function. However, there is a constraint: for a specific parameter (a, b, or c), a specific equation must be satisfied.

## V. Simulation Results and Analysis

After introducing of VOC and DPC methods for applying on the three-phase rectifier, and design of the ANFIS

controller, we use this controller in both methods, as voltage controller block, and presented the output of the simulations. Finally results are compared to the situation that PID controller is applied as voltage controller in VOC and DPC methods.

Whole of the design process is performed in the MATLAB/SIMULINK environment. As mentioned previously, the universal 6-switch bridge model of the switching rectifier is applied for both VOC and DPC methods. Also, control block of the VOC and DPC controllers are presented in Fig. 8.

### A. ANFIS controller in VOC method

For this part of simulation, the VOC method is simulated. Fig. 9 presents this strategy in the SIMULINK. The proposed ANFIS controller applied as voltage controller block, and current controller blocks for d and q axis (same as Fig. 3), use PID controllers which are designed according to the procedure described in [3]. The learning rate of the coefficient of the ANFIS is set to  $\eta=0.0003$ . In this system, output DC voltage is set to 400V. A resistive load of 250Ω is connected to the DC link. In order to examine the load regulation capability of the rectifier, a 750Ω resistive load is paralleled to primary 250Ω load using one breaker during simulation. To evaluate the PID controller performance, a controller that its parameters are designed according to [3], is used as voltage controller. Two decoupled current controllers' parameters are similar in both PID and ANFIS-based controllers.

In Fig. 10 (a,b), output DC voltage of the rectifier, and also input voltage and current of the rectifier is shown, and the ANFIS controller is applied for controlling of the system. In Fig. 11 (a,b), this simulations is repeated when PID controller is used as the controller of the system. It should be mentioned that the input current of the rectifier is multiplied by 10.

From simulation results it is obvious that the VOC-based controlling system of the Three-phase rectifier, when using the ANFIS controller, has lower ripple and shorter settling time in both output voltage and current in comparison with PID controller. Also, the sudden variation in the output load has little effect on the operation of the system when using the ANFIS controller and this controller can adapted rapidly with the new condition. Furthermore, when ANFIS is used, input voltage and current of the rectifier are absolutely in phase and it has no reactive power exchanging with grid. Numerical comparison is presented in the table III, between ANFIS and PID controllers for VOC application.

### B. ANFIS controller in DPC method

In this section, DPC is simulated based on the previous description of this method. Fig. 12 presents this strategy in

SIMULINK. ANFIS controller applied as a voltage controller block of the Fig. 5. The learning rate of the coefficient of the ANFIS is set to  $\eta=0.0007$ . Rectifier

features and also scenario of examining the load regulation capability are same a previous simulation.

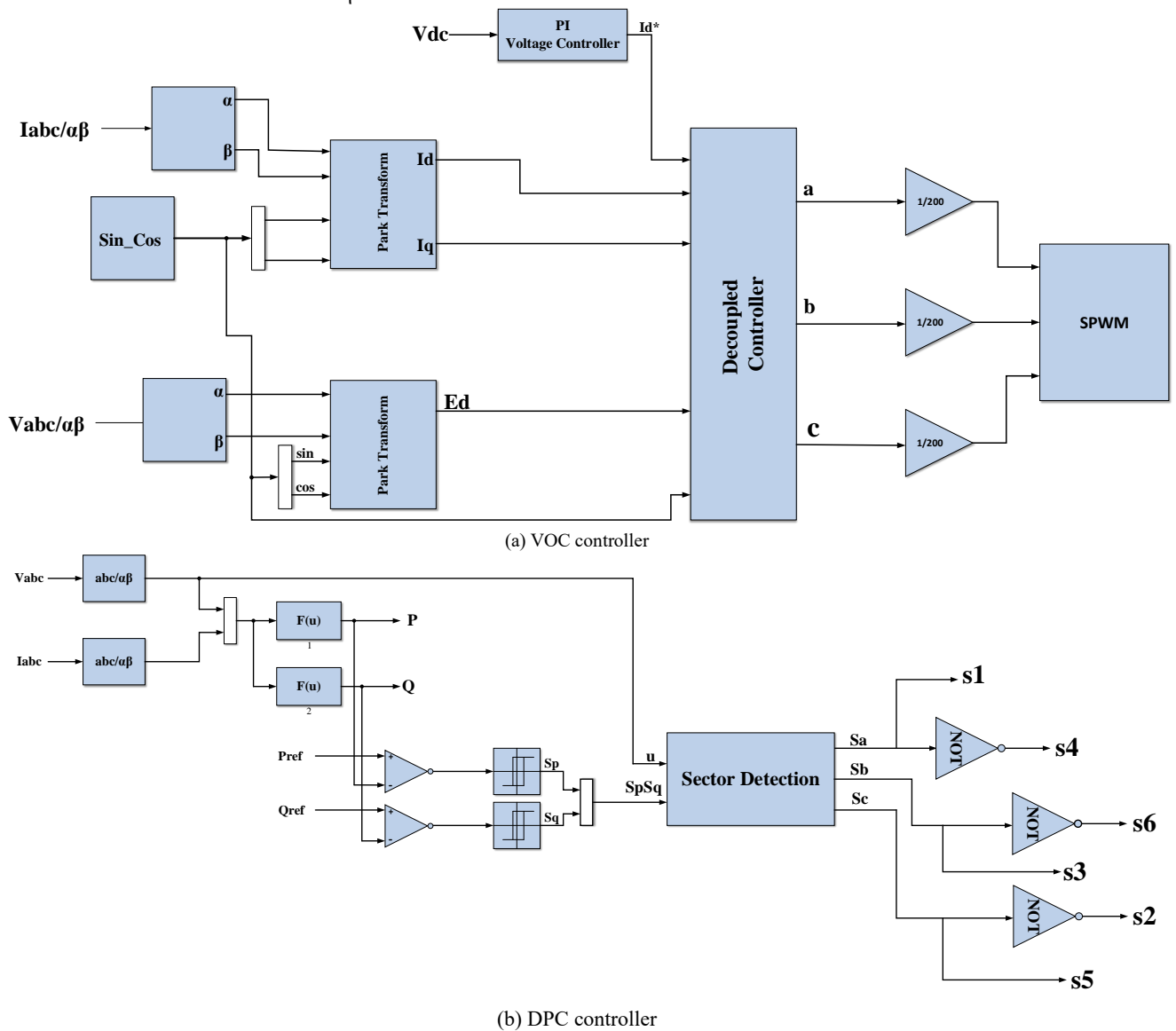


Fig. 8. Block diagram of the VOC and DPC controller in SIMULINK.

To evaluate the PID controller performance, a controller that its parameters are designed according to [3], is used as a voltage controller instead of the voltage controller unit in the DPC system.

In Fig. 13 (a,b), output DC voltage of the rectifier, input voltage and current of the rectifier, are demonstrated. The proposed ANFIS system is applied for controlling of the system. In Fig. 14 (a,b) this work is repeated when PID controller is used as controller. It should be considered that the input current of the rectifier is multiplied by 10.

From simulation results it is clear that the DPC-based controlling system of the three-phase rectifier, when using the ANFIS controller, has lower ripple and shorter settling time in output voltage in comparison with PID controller. Also it can be found that the sudden changes in the output load has the few effect on the operation of the system when using the proposed ANFIS and this controller can adapted with the new condition. Also when ANFIS is used, input voltage and current of the rectifier are absolutely in phase and it has no reactive power exchanging with grid. Numerical comparison is shown in the table IV, between ANFIS and PID controllers for DPC application

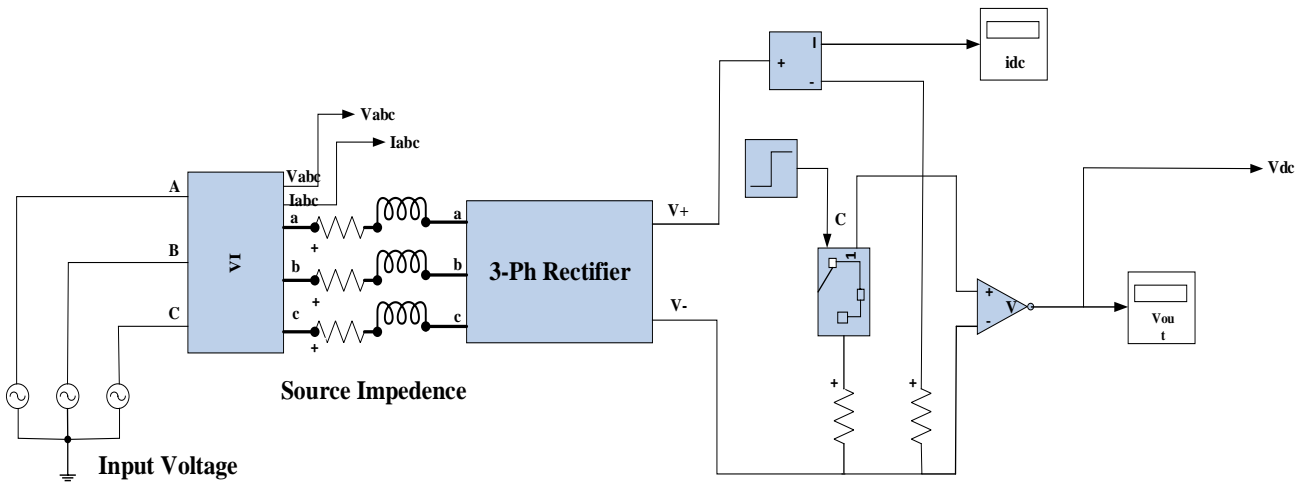
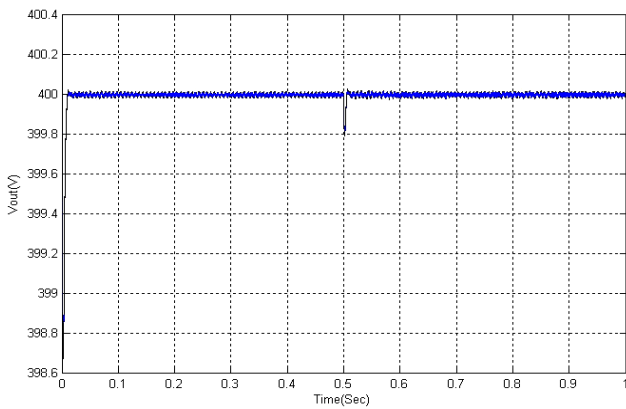
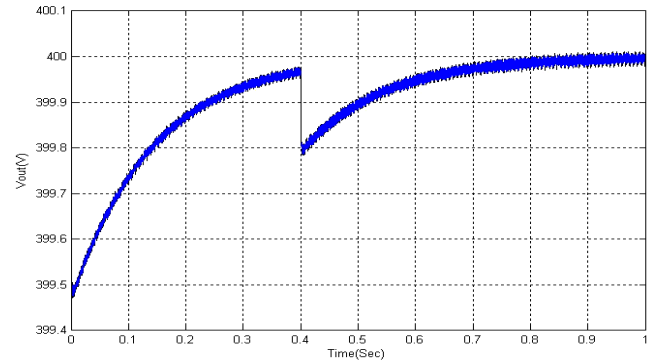


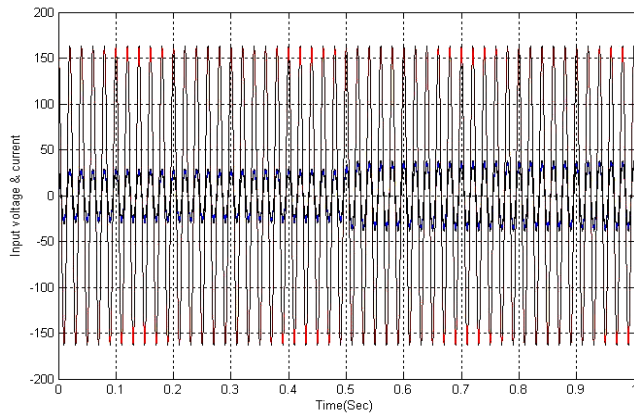
Fig. 9. Block diagram of the VOC method in SIMULINK.



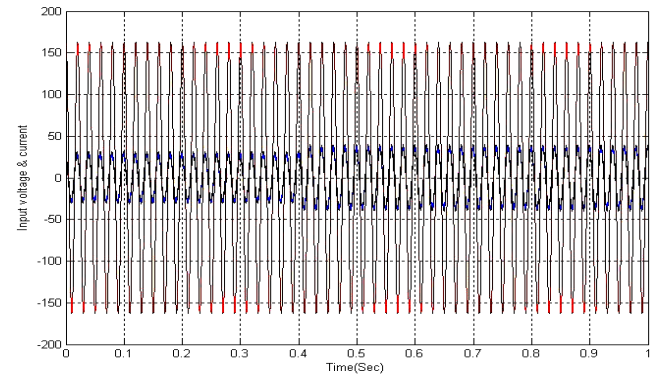
(a) Output DC voltage



(a) Output DC voltage



(b) Input voltage and current (blue is current, red is voltage)



(b) Input voltage and current (blue is current, red is voltage)

Fig.10. Output DC voltage of the rectifier, and also input voltage and current of the rectifier, when the ANFIS controller is applied for controlling of the VOC-based system

Fig. 11. Output DC voltage of the rectifier, and also input voltage and current of the rectifier, when the PID controller is applied for controlling of the VOC-based system.

TABLE III COMPARISON OF UNDERSHOOT AND SETTLING TIME BETWEEN ANFIS AND PID CONTROLLERS FOR VOC METHOD.

| Works (Parameters)               | Undershoot | Settling time |
|----------------------------------|------------|---------------|
| PID<br>(DC output voltage)       | 0.15%      | 0.5s          |
| ANFIS<br>(DC output voltage)     | 0.25%      | 0.02s         |
| PID<br>(DC output current)       | 0.002%     | 0.05s         |
| ANFIS<br>(DC output current)     | 0.001%     | 0.01s         |
| PID<br>(output voltage ripple)   |            | 0.03V         |
| ANFIS<br>(output voltage ripple) |            | 0.02V         |

TABLE IV COMPARISON OF OVERSHOOT AND SETTLING TIME BETWEEN ANFIS AND PID CONTROLLERS FOR DPC METHOD.

| Works (Parameters)               | Undershoot | Settling time |
|----------------------------------|------------|---------------|
| PID<br>(DC output voltage)       | 0.125%     | 0.12s         |
| ANFIS<br>(DC output voltage)     | 0.03759%   | 0.3s          |
| PID<br>(output voltage ripple)   |            | 0.01V         |
| ANFIS<br>(output voltage ripple) |            | 0.005V        |

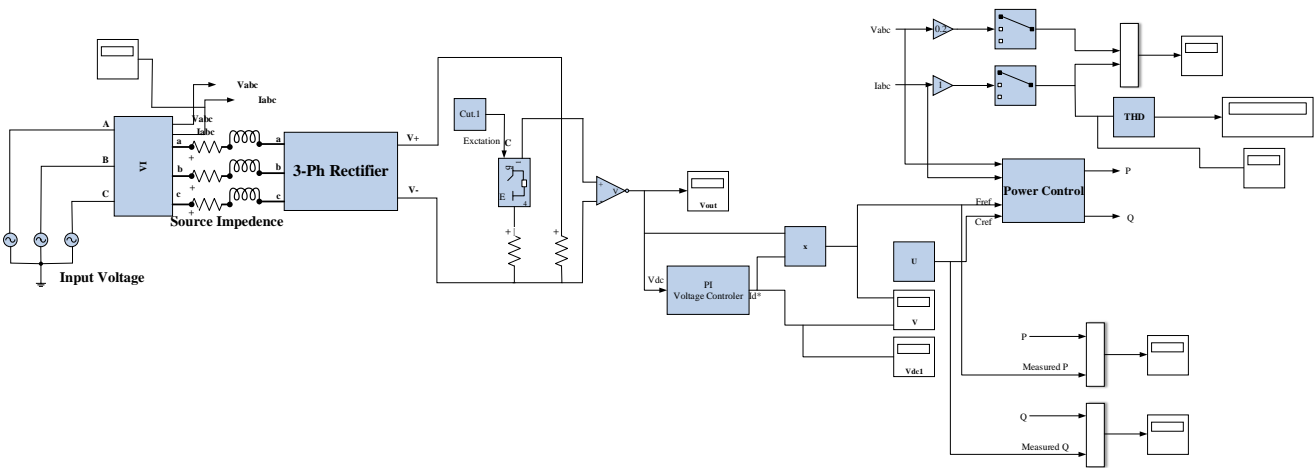
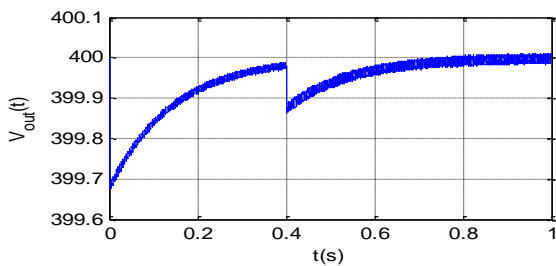
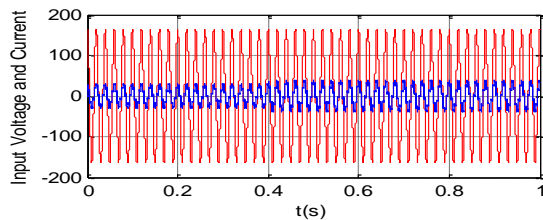


Fig. 12. Block diagram of the DPC method in SIMULINK.

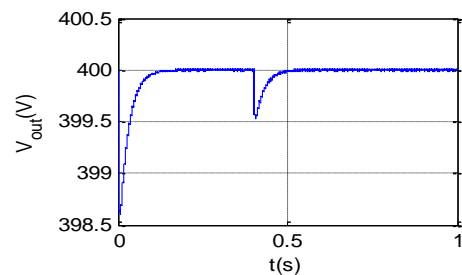


(a) Output DC voltage

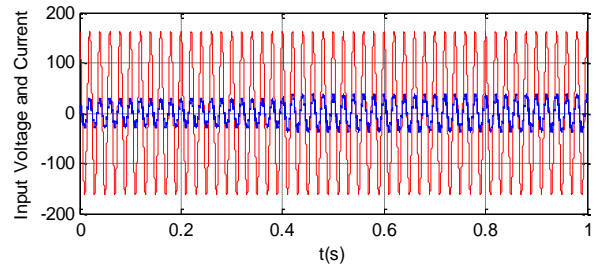


(b) Input voltage and current (blue is current, red is voltage)

Fig. 13. Output DC voltage of the rectifier, input voltage and current of the rectifier, when the ANFIS controller is applied for controlling of the DPC-based system.



(a) Output DC voltage



(b) Input voltage and current (blue is current, red is voltage)

Fig. 14. Output DC voltage of the rectifier, input voltage and current of the rectifier of rectifier, when the PID controller is applied for controlling of the DPC-based system.

## VI. Conclusion

This paper proposed a novel hybrid intelligent controller for 6-switch three-phase PWM rectifiers. This Adaptive Neuro-Fuzzy Inference System (ANFIS) controller utilizes the strengths of both FL and NNs to enhance the static and dynamic performance of Voltage Oriented Control (VOC) and Direct Power Control (DPC) methods. The fuzzy control process is implemented through a specifically designed 5-layer NN architecture. This architecture facilitates the implementation of the fuzzy control strategy. The network has 2 nodes in the first layer, 14 nodes in the second, 49 nodes in both the third and fourth layers, and finally 1 node in the output layer. The learning process utilizes the Forward Signal and Backward Error Back-Propagation (FSBEBP) algorithm. FSBEBP relies on a single error signal to propagate adjustments throughout the network, for effectively updating the parameters within the ANFIS structure.

## REFERENCES

- [1] N. Nandola, B. Wang, X. Wu, R. Burgos, "Control of DC Microgrid Based flexible Cold-Rolling Steel Mill Plant – an Application of Grid Supporting Rectifier," IEEE 24th Workshop on Control and Modeling for Power Electronics (COMPEL), pp.1-7, 2023.
- [2] A. Zhetessov, G. Venkataramanan, "Systematic Adaptive Robust State Feedback Control for Active Front-End Rectifiers," 2022 24th European Conference on Power Electronics and Applications (EPE'22 ECCE Europe), pp.1-11, 2022.
- [3] A. Khan, M. Hosseinzadehtaher, M. B. Shadmand, S. Bayhan, H. Abu-Rub, "On the Stability of the Power Electronics-Dominated Grid: A New Energy Paradigm," IEEE Industrial Electronics Magazine, vol.14, no.4, pp. 65-78, 2020.
- [4] C. M. Emeghara, S. M. Mahajan, A. Arzani, "Direct Power Control of a Surface-Mounted Permanent Magnet Synchronous Generator Wind Turbine for Offshore Applications," IEEE Access, vol.11, pp. 62409-62423, 2023.
- [5] W. Ende and H. Shenghua, "Robust Control of the Three-Phase Voltage-Source PWM Rectifier Using EKF Load Current Observer," Journal of Electrical Review, R. 89, pp. 189-193, NR 3a/2015.
- [6] J. Hu, L. Shang, Y. He, and Z. Q. Zhu, "Direct Active and Reactive Power Regulation of Grid-Connected DC/AC Converters Using Sliding Mode Control Approach," IEEE Trans. Power Electron., vol. 26, no. 2017.
- [7] S. Maganti, N. P. Padhy, "Analysis and Design of PLL Less Current Control for Weak Grid-Tied LCL-Type Voltage Source Converter," IEEE Journal of Emerging and Selected Topics in Power Electronics, vol.10, no.4, pp. 4026-4040, 2022
- [8] S. Samanta, S. Barman, J. P. Mishra, P. Roy, B. K. Roy, "Design of an Interconnection and Damping Assignment-Passivity Based Control Technique for Energy Management and Damping Improvement of a DC Microgrid," IET Generation, Transmission & Distribution, vol.14, no.11, pp. 2082-2091, 2020.
- [9] Y. Gui, C. Kim, C. C. Chung, J. M. Guerrero, Y. Guan, and J. C. Vasquez, "Improved Direct Power Control for Grid-Connected Voltage Source Converters," IEEE Trans. Ind. Electron., vol. 65, no. 10, pp. 8041–8051, 2018.
- [10] L. Tai, M. Lin, H. Li, Y. Li, "A Novel Three-Vector-Based Model Predictive Direct Power Control for Three-Phase PWM Rectifier," Electronics, 10 (21), Article number: 2579, 2021.
- [11] J. Jang, "Self-Learning Fuzzy Controller Based on Temporal Back-Propagation," IEEE Transaction on Neural Network, Vol. 3, pp.714-723, September 1992.
- [12] A. Kumar and G. Srungavarapu "A Novel Voltage Sensorless DPC Approach of AFE Rectifier Based on Virtual Flux and Dynamic DC Link Reference Design," 2016 IEEE Annual India Conf. (INDICON), Bangalore, 2016, pp. 1–6
- [13] A. Baktash, A. Vahedi, and M. A. S. Masoum "New Switching Table for Improved Direct Power Control of Three-Phase PWM Rectifier," Aust. J. Electr. Electron. Eng., 2015, 5, (2), pp. 161–167.
- [14] C. Lin and Y. Lu, "A Neural Fuzzy System with Fuzzy Supervised Learning," IEEE, Transaction on Systems, Man and Cybernetics, Vol. 26, No. 5, October 1996.
- [15] M. R. Mosavi, A. Rahmati and A. Khoshsaadat, "Design of Efficient Adaptive Neuro-Fuzzy Controller Based on Supervisory Learning Capable for Speed and Torque Control of BLDC Motor," PRZEGLĄD ELEKTROTECHNICZNY (Electrical Review), Vol. 88, pp. 238-246, 2012.
- [16] S. Tano, T. Oyama and T. Arnould, "Deep Combination of Fuzzy Inference and Neural Network in Fuzzy Inference, Journal on Fuzzy Sets and Systems, Vol. 82, No. 2, pp.151-160, 1996.
- [17] T. Takagi and M. Sugeno, "Fuzzy Identification of Systems and its Applications to Modeling and Control," IEEE Transaction. On Systems, Man and Cybernetics, Vol. 15, pp. 116-132, 1985.
- [18] A. Khoshsaadat, M. R. Mosavi, J. S. Moghani, A. Khoshooei, "Design of a Controller with ANFIS Architecture Attendant Learning Ability for SSSC-Based Damping Controller Applied in Single Machine Infinite Bus System," Iranian Journal of Electrical and Electronic Engineering (IJEEE), Vol. 10, No. 3, pp. 212-222, 2014.
- [19] Y. Q. Zhang, and A. Kandel, "Compensatory Neuro-Fuzzy Systems With Fast Learning Algorithms," IEEE Transaction on Neural Networks, Vol. 9, No. 1, January 1998.
- [20] R. Zaheri, A. Khoshsaadat, J. S. Moghani, M. Abedi, "Fast Transient Hybrid Neuro-Fuzzy Controller for STATCOM During Unbalanced Voltage Sags," AUT Journal of Electrical Engineering, Vol. 50, No. 1, pp. 67-74, 2018.
- [21] R. Sivakumar, C. Sahana, P. A. Savitha, "Design of ANFIS-Based Estimation and Control for MIMO Systems," International Journal of Engineering Research

and Applications, Vol. 2, Issue 3, pp. 2803-2809, May-Jun 2012.

- [22] T. C. Lin and C. S. Lee, "Neural Network Based Fuzzy Logic Control and Decision System," IEEE Transactions on Computers, Vol.40, No.12, pp.1320-1336, December 2009.



**Alireza Khoshsaadat** was born in Boroujerd, Iran, in 1986. He received his B.Sc. degree in Electrical Engineering (EE) from Shahid Beheshti University (SBU), Tehran, Iran, in 2009, his M.Sc. degree in EE from Iran University of Science and Technology (IUST), Tehran, Iran, in 2011, and his Ph.D. degree in EE from Amirkabir University of Technology (AUT), Tehran, Iran, in 2018. He is currently a faculty member at department of electrical engineering in Shahid Beheshti University (SBU), Tehran, Iran, as an assistant professor. His research interests include analysis, design and development of power electronics converters especially with the approach of application in Electric Vehicle (EV) subsystems and chargers.



**Arash Khoshoeei** received the B.Sc. degree in Electrical Engineering (EE) from Shahid Chamran University, Ahvaz, Iran, in 2002, and the M.Sc. degree in EE from Amirkabir University of Technology (AUT), Tehran, Iran, in 2004. He joined as a lecturer to Jundi-Shapur University of Technology (JSU), Dezful, Iran in 2005. He received the PhD degree in Power Electronics from AUT in 2018. During 2015 to 2016, he was a visiting student at the Technical University of Catalonia (UPC), Barcelona, Spain. In 2018 he backed to JSU as an assistant professor. His research interests include modeling and control of power electronics converters and integration of distributed generation systems.



**Mohammad Abedini** was born in Boroujerd, Iran, in 1986. He received his B.Sc. degree in electrical engineering from the Islamic Azad University of Ayatollah Boroujerdi, Iran, in 2006, and his M.Sc. and Ph.D. degrees in electrical engineering from Bu-Ali Sina University in 2008 and 2010, respectively. He is currently an associate professor at Ayatollah Boroujerdi University. His current research interests include microgrids and distribution systems.



**Mohammadreza Mirzaei** was born in Boroujerd, Iran, in 1999. He holds a bachelor's degree in Power Engineering from Ayatollah Boroujerdi University and is currently pursuing a master's degree at the same university, specializing in Planning and Management of Electrical Energy Systems. His research interests include planning and optimization of electrical energy systems.